Using generative adversarial networks (GAN) to simulate central-place foraging trajectories

Amédée Roy, Ronan Fablet, Sophie Lanco Bertrand

Received: 29 September 2021 | Accepted: 25 February 2022

DOI: 10.1111/2041-210X.13853

Methods in Ecology and Evolution BRITISH ECOLOGICAL SOCIETY

RESEARCH ARTICLE

Using generative adversarial networks (GAN) to simulate central-place foraging trajectories

Amédée Roy[1] | Ronan Fablet[2] | Sophie Lanco Bertrand[1]

[1]Institut de Recherche pour le Développement (IRD), MARBEC (Univ. Montpellier, Ifremer, CNRS, IRD), Sète, France

[2]IMT Atlantique, UMR CNRS Lab-STICC, Brest, France

Correspondence
Amédée Roy
Email: amedee.roy@ird.fr

Funding information
Agence Nationale de la Recherche; Centre National d'Etudes Spatiales; Horizon 2020 Framework Programme, Grant/Award Number: 817578; Institut de Recherche pour le Développement; LEFE Program

Handling Editor: Edward A Codling

Abstract

1. Miniature electronic devices have recently enabled ecologists to document relatively large amounts of animal trajectories. Modelling such trajectories may contribute to explaining the mechanisms underlying observed behaviours and to clarifying ecological processes at the scale of the population by simulating multiple trajectories. Existing approaches to animal movement modelling have mainly addressed the first objective, and are often limited when used for simulation purposes. Individual-based models generally rely on ad hoc formulation and their empirical parametrization lacks generability, while random walks based on mathematically sound statistical inference typically consist of first-order Markovian models calibrated at the local scale which may lead to overly simplistic description and simulation of animal trajectories.
2. We investigate a recent deep learning tool—generative adversarial networks (GAN)—to simulate animal trajectories. GANs consist of a pair of deep neural networks that aim to capture the data distribution of some experimental dataset. They enable the generation of new instances of data that share statistical properties. This study aims at identifying relevant deep network architectures to simulate central-place foraging trajectories, as well as at evaluating GANs drawbacks and benefits over classical methods, such as state-switching hidden Markov models (HMM).
3. We demonstrate the outstanding ability of deep convolutional GANs to simulate and to capture medium- to large-scale properties of seabird foraging trajectories. GAN-derived synthetic trajectories reproduced the Fourier spectral density of observed trajectories better than those simulated using HMMs. However, unlike HMMs, GANs do not adequately capture local-scale descriptive statistics, such as step speed distributions.
4. GANs provide a new likelihood-free approach to calibrate complex stochastic processes and thus open new research avenues for animal movement modelling. We discuss the potential uses of GANs in movement ecology and future

developments to better capture local-scale features. In this context, embedding HMM-based priors in GAN schemes appears as a promising research direction.

KEYWORDS
animal telemetry, deep learning, hidden Markov model, movement model, seabird

1 | INTRODUCTION

Recent advances in telemetry enabled ecologists to track free-ranging animals and to gather large trajectory datasets (Chung et al., 2021; Ropert-Coudert et al., 2009). GPS recorders have been at the forefront of this breakthrough and can now provide accurate data on the movements of many species, such as mammals (McMahon et al., 2017), seabirds (Yoda, 2019) and many other large-sized vertebrate (Kays et al., 2015). These movement data contain crucial information about animal behaviour, including habitat selection, migration patterns and foraging strategies but present key challenges for movement ecologists to explain underlying animal movement ecology (Nathan et al., 2008).

Since the movement processes of many animals are relatively poorly known, simulation of trajectories is fundamental to tracking data analysis. Trajectory simulations have notably served as a null model for testing various hypotheses concerning movement (Zurell et al., 2010). For instance, they have been used to generate pseudo-absences in a habitat selection model (Hückstädt et al., 2020), to illustrate the effect of prey distribution on foraging movements (Boyd et al., 2017) and to demonstrate the effectiveness of social interactions (Bastos et al., 2020). Moreover, for practical and ethical considerations, the tracking of large numbers of individuals is not often possible. Simulated trajectories provide a relevant alternative to develop methods based on synthetic data; for example, to correct bias in home range estimation (Winner et al., 2018) or for assessing the impact of sample size (Sequeira et al., 2019). Simulation tools may also be of interest in data pre-processing, such as filling gaps and upscaling the temporal resolution of movement data (Michelot & Blackwell, 2018).

Animal trajectories are generally seen as a succession of elementary movement events called steps (Nathan et al., 2008), and the use of random walks (RW) has received increased attention to describe step sequences (Codling et al., 2008). This includes correlated RW (e.g. Bergman et al., 2000), Lévy RW (e.g. Viswanathan et al., 2008), state-space models (e.g. Patterson et al., 2008) and stochastic differential equations (e.g. Johnson et al., 2008). RWs have also been used as 'building blocks' for more complex models to simulate realistic global animal movement patterns. To this end, behavioural heterogeneity is often taken into account by developing state-switching models where animal movements are seen as the outcome of distinct behavioural modes (e.g. travelling, resting and foraging) (Morales et al., 2004). This is notably enabled by discrete multistate RWs such as hidden Markov models (HMM) (McClintock et al., 2012; Michelot et al., 2017) and by continuous-time multistate correlated RWs (Johnson et al., 2008; Michelot & Blackwell, 2018). The main advantages of continuous-time approaches are that they do not depend on sampling resolution and that they can deal with irregularly sampled data. Discrete-time models are still an important tool since they are more intuitive and can better handle more than two behavioural modes (McClintock et al., 2014). The modelling and simulation of central-place foraging trajectories (CPFT), such as those of seals (Michelot et al., 2017), seabirds (Pirotta et al., 2018) and wolves (Ylitalo et al., 2021), are typical applications of discrete-time HMM methods. The fundamental characteristic of central-place foragers is that individuals must return regularly to their central location, and thus perform looping foraging trips. By defining an 'inbound' behavioural mode dedicated to returning home, previously cited studies managed to describe loop-shaped foraging trips.

The above-mentioned statistical movement models are mainly fitted through likelihood maximization or Bayesian statistics (Hartig et al., 2011). They can, however, suffer from challenging parameter estimation, especially as models increase in complexity (e.g. high number of behavioural modes and covariates) (Adam et al., 2019; Michelot et al., 2017). For these reasons, the simulation of CPFTs is also performed using RWs embedded within empirically parametrized individual-based models (IBM). IBMs aim to explicitly represent the interactions between individuals and their environment based on ad hoc formulations, and they provide a pragmatic way to simulate nonlinear movement processes (DeAngelis & Grimm, 2014). For example, some studies embed HMM (e.g. Boyd et al., 2017), correlated RW (e.g. Massardier-Galatà et al., 2017) or mixtures of random and deterministic movement (Barraquand et al., 2009) in IBMs for the simulation of CPFTs. They, however, often lack generability, have intractable likelihood and are not always directly calibrated from observed data. There has been much work to address these issues, and to parameterize IBMs using likelihood-free methods (Grimm et al., 2005; Hartig et al., 2011). In particular, there is a growing interest for data-driven approaches, such as deep learning techniques, in order to calibrate complex ecological systems (Malde et al., 2020).

Deep learning refers to neural networks with multiple layers of processing units (LeCun et al., 2015). By decomposing the data into these multiple layers, deep neural networks allow learning complex features to represent the data with high level of abstraction at multiple scales. Recently, deep learning tools have demonstrated their great ability to simulate complex systems using generative adversarial networks (GAN) (Goodfellow et al., 2014). GANs consist in a pair of deep neural networks that aim to capture the data distribution of some experimental dataset, and that enable to generate new

instances of data that share statistical properties. It has become a state-of-the-art approach to generate various types of data, such as image, audio and spatio-temporal data including human trajectories (Cao et al., 2019; Gao et al., 2020).

This paper investigates GANs for the simulation of animal trajectories, and more particularly CPFTs. Our key contributions are the design of different GAN architectures and the evaluation of GANs benefits over 'state-of-the-art' tools, that is state-switching HMM. We further discuss the pros and cons of GANs with respect to HMMs, along with the research avenues opened by GANs to address contemporary ecological challenges.

2 | MATERIALS AND METHODS

2.1 | Generative adversarial networks

2.1.1 | Background

The location of an animal is generally represented by a time-continuous or discrete-time stochastic process $(X_t)_{t\geq 0}$, where t denotes time. A Markovian hypothesis is classically stated for this movement process, assuming that one can fully predict the distribution of the future state of an animal given its current state (Patterson et al., 2008). This hypothesis can only be regarded as an approximation of real movement patterns, which generally also involve long-term dependencies due to factors such as perceptual ranges, memory, social interactions, etc. The calibration of these models generally relies on the maximization of the likelihood of observed trajectories at local scales. It typically comes to estimating the joint distribution of step length and turning angle from GPS tracks.

A wide range of probabilistic models can be restated as the composition of a deterministic function G and of the sampler of a random latent variable. We may illustrate this point for correlated RW as presented in Patterson et al. (2008). Let us denote by s_t and ϕ_t the step length and the turning angle, respectively, at time t. The correlated RW can be written as follows:

$$\begin{pmatrix} (s_1,\phi_1) \\ \vdots \\ (s_n,\phi_n) \end{pmatrix} = \begin{pmatrix} (F^{-1}(z_G^1|\theta_F),H^{-1}(z_H^1|\phi_0,\theta_H)) \\ \vdots \\ (F^{-1}(z_G^n|\theta_F),H^{-1}(z_H^n|\phi_{n-1},\theta_H)) \end{pmatrix} = G(z), \quad (1)$$

where F and H are cumulative density functions with parameters θ_F and θ_H, often chosen as log-normal and von Mises distributions, and where z_G^i and z_H^i are independent samples from the uniform distribution over [0, 1].

The generative model in a GAN also relies on the application of a deterministic function G to random samples of a latent variable z, according to a predefined distribution. Function G is chosen within a parametric family of differentiable functions and implemented as a neural network for flexibility. The other major difference with statistical inference approaches classically exploited in movement ecology lies in the calibration approach from data. Rather than using an explicit likelihood criterion, the calibration of the generator of a GAN involves the simultaneous training of another deep network D (referred to as the discriminator) that learns how to distinguish simulated data (i.e. $G(z)$) from real data. The typical architecture of a GAN is given in Figure 1a. If no discriminator can distinguish the simulated and real data, it means that the generator truly samples the unknown distribution of the training dataset (Goodfellow et al., 2014).

2.1.2 | Network architecture

Numerous deep network architectures can be used for both the generator and discriminator networks. Long short-term memory (LSTM) networks and convolutional neural networks (CNNs) are probably the most popular, efficient and widely used deep learning techniques (Alom et al., 2019). In this study, we used two architectures for the generator and the discriminator, namely CNN-based and LSTM-based architectures (see Figure 2). Here, we briefly present the motivation of these networks and how they function. We refer the reader to Christin et al. (2019) for a detailed introduction to deep networks.

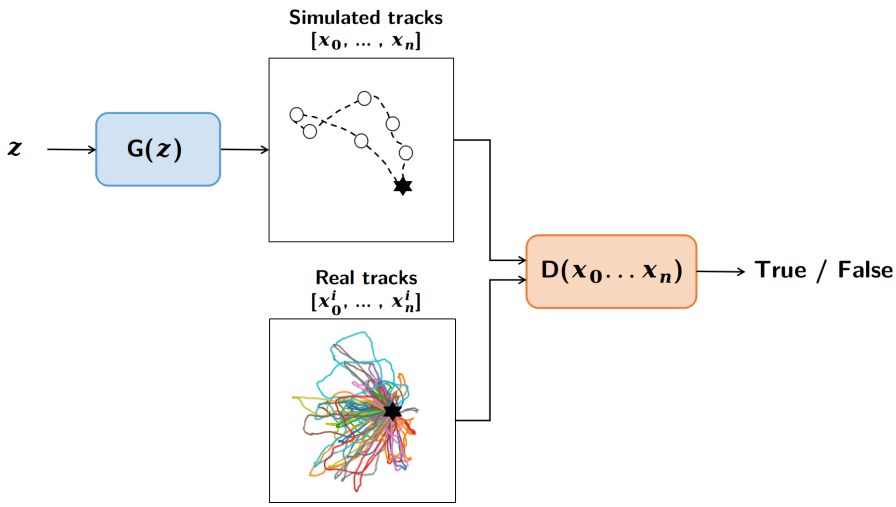

FIGURE 1 GAN architecture: Global architecture of a generative adversarial network. G refers to the generator network that takes as input a random noise vector z and outputs a trajectory x. D is the discriminator network that aims at distinguishing real trajectories from simulated ones

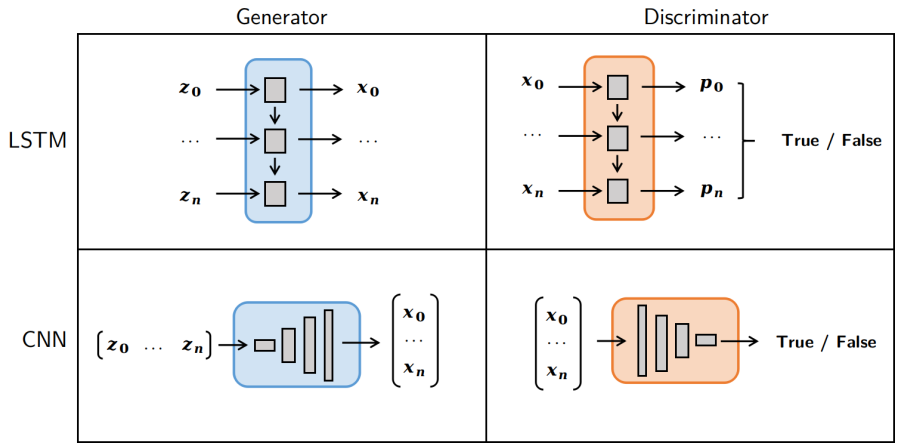

FIGURE 2 LSTM versus CNN: Architecture of LSTM and CNN networks used in this study

LSTM

Long short-term memory networks are among the state-of-the-art architectures of recurrent neural networks dedicated to the modelling of time series, including trajectories. A key feature of LSTM is its ability to identify and exploit long-term dependencies through gating processes (Alom et al., 2019). LSTM-based architecture has also been used in numerous recurrent GANs for pedestrian trajectory and medical time-series generation (e.g. Esteban et al., 2017; Gao et al., 2020).

In our study, we used a generator network composed of a LSTM layer that takes a different random seed at each temporal input, and produces a sequence of hidden vectors with 16 features. These hidden vectors encode the state of the trajectory. An additional dense layer maps the 16-dimensional hidden vector at a given time step to the corresponding longitudinal and latitudinal displacements. We derive a time series of positions from the cumulative sum of these elementary displacements (see Figure 2).

We can also exploit a LSTM for the discriminator. Given a sequence of positions (longitude, latitude), the LSTM acts as an encoder of this sequence in some higher dimensional latent space. A dense layer was then applied to assign a probability to being realistic at each position of the sequence. Overall, the output of the discriminator is the associated mean probability to assess the quality of the whole trajectory (see Figure 2).

CNN

CNN architectures exploit convolutional layers and are the state-of-art architectures for a wide range of applications, especially for signal and image processing tasks. They are particularly effective in extracting low-level and high-level features from n-dimensional tensors (Alom et al., 2019).

CNN are also widely exploited in GANs (Radford et al., 2016). Here, we follow the general architecture proposed in Radford et al. (2016) for image generation. The generator takes as input a random noise vector that can be seen as a latent representation of a global time series. It then applies a series of successive fractional-strided convolutions to map the latent representation into time series with increasing numbers of points and decreasing numbers of features, until it outputs a two-dimensional vector of the required length (see Figure 2). In our work, we used a batchnorm and a ReLU activation after each fractional-strided convolution, except for the output that used only a hyperbolic tangent, as suggested by Radford et al. (2016)). We may point out that, in this CNN architecture, there is no explicit sequential modelling of the trajectory and that the latent representation may not be time related.

Regarding the CNN-based discriminator, we also applied successive strided convolutions in order to transform the initial trajectory into time series with decreasing lengths and increasing numbers of features, until we obtained a latent vector describing the whole trajectory. We used batchnorm and a LeakyReLU activation after every strided convolution. The last layer is a dense layer with a sigmoid activation that transforms the latent representation into a probability for the trajectory of being realistic (see Figure 2).

2.1.3 | Adversarial training and spectral regularization

For a given architecture, networks' parameters are estimated using adversarial training, that is the two networks compete in a minimax two-player game given by Equation 2. Discriminator D is trained to maximize the probability of assigning the correct label to both training examples and samples from G, that is to maximize $\log D(x) + \log(1 - D(G(z)))$. Generator G is simultaneously trained to fool the discriminator, that is to minimize $\log(1 - D(G(z)))$.

$$\min_G \max_D \mathbb{E}_{x\sim p_{\text{data}}(x)}\left[\log D(x)\right] + \mathbb{E}_{z\sim p_z(z)}\left[\log(1 - D(G(z)))\right]. \quad (2)$$

Numerically, we apply stochastic gradient descents over the discriminator and generator successively where at each iteration, we compute the training losses for a randomly sampled subset of m trajectories within the training dataset[1]:

$$\mathscr{L}_{\text{discriminator}} = \frac{1}{m}\sum_m \left[\log(D(x)) + \log(1 - D(G(z)))\right],$$
$$\mathscr{L}_{\text{generator}} = \frac{1}{m}\sum_m \log(D(G(z))). \quad (3)$$

We may complement the training loss of the generator with additional terms, including both application-specific (Ledig et al., 2017) and regularization (Durall et al., 2020) terms. In particular, recent studies have demonstrated that a spectral regularization may have positive effects, both on the training stability and the output quality of generative networks for image simulation (Durall et al., 2020). We tested here a similar approach with the following spectral loss L_{spectral} to the generator's gradient descent:

$$\mathscr{L}_{\text{spectral}} = \sum \left[\log\left(F\left(x_0, \ldots, x_n\right)\right) - \log\left(F\left(\hat{x}_0, \ldots, \hat{x}_n\right)\right)\right]^2, \quad (4)$$

where F is the module of the Fourier transform of a two-dimensional time series, x and $\hat{x}$ are real and simulated trajectories respectively.

2.2 | Case studies and experiments

2.2.1 | Datasets

GPS recorders were fitted to tropical boobies during their breeding period at the Pescadores Island, Peru in from 2008 to 2013, and at the Fernando de Noronha archipelago, Brazil, from 2017 to 2019 (Table 1). This work was conducted with the approval of the Peruvian federal agency, Programa de Desarrollo Productivo Agrario Rural, commonly known as 'Agrorural'. Headquarters of Agrorural are located at Av. Salaverry 1388, Lima, Peru, and of the Brazilian Ministry of Environment—Instituto Chico Mendes de Conservação da Biodiversidade (Authorization No 52583-5). Trajectories consist in foraging trips where seabirds look for preys at sea and come back to their colony. Data points have been linearly re-interpolated at regular time steps, and coordinates have been centred on the colony's location and normalized. In particular, red-footed booby tracks were substantially downsampled in order to provide a simplistic dataset on which to evaluate distinct GAN architectures (see Table 1). Finally, trajectories have been padded with zeros so that all longitude/latitude time series from a dataset would have the same length.

2.2.2 | Architecture selection experiment

We first designed an experiment to compare different GAN architectures. For this experiment, we considered the simplest dataset with a 1-hr time resolution (see Table 1). All trajectories involved 20 time steps. We evaluated four different GAN corresponding to every generator-discriminator pair for the considered CNN and LSTM architectures; for example, we call 'LSTM-CNN' the GAN with a LSTM network as generator and a CNN as discriminator.

For all generators, the input random noise vector consisted of 20 samples from a uniform distribution on $[0, 1]$. We trained all networks over 5,000 epochs with a learning rate of 2e-4 using the loss functions given in Equation 3. The score of each approach was assessed by computing the mean squared error of the logarithmic Fourier decomposition spectrum of simulated and real trajectories, $\mathscr{L}_{\text{spectral}}$ (see Equation 4).

TABLE 1 Datasets' overview with trajectories from red-footed booby *Sula sula*, masked booby *Sula dactylatra* and Peruvian booby *Sula variegata*

Species	Country	No. trips	Resolution	Padding
Sula sula	Brazil	30	1 hr	20 steps
Sula dactylatra	Brazil	50	5 min	200 steps
Sula variegata	Peru	78	1 min	200 steps

2.2.3 | GAN versus HMM experiment

In this section we compared the best GAN architecture from the previous experiment, namely 'CNN-CNN' GAN architecture, to a state-switching HMM. We tested both methods on the two datasets with 200-step time series consisting in trajectories of tropical boobies from two completely distinct ecosystems and with different foraging strategies (see Table 1).

GAN

The input random noise vector consisted in 256 samples from a uniform distribution on $[0, 1]$. We trained the 'CNN-CNN' GAN architecture separately on each dataset over 5000 epochs and with a learning rate of 2e-4. We used a spectral regularization to better reproduce the spectral features of real trajectories, especially for fine time-scales, and to increase learning stability.

HMM

For comparison, we fitted a 'state-of-the-art' state-switching HMM to seabirds CPFTs. We followed the methodology presented by Michelot et al. (2017), which relies on a rigorous statistical inference.

Movements were described as a sequence of step lengths and turning angles that we fitted with gamma distribution and von Mises distribution respectively. Three behavioural modes were used for the Peruvian datasets, that is 'searching', 'foraging' and 'inbound', while a fourth mode, 'resting', was added with the Brazilian dataset (Figure 5). For the modes of 'searching', 'foraging' and 'resting', we described movement as correlated RW, while for the mode 'inbound' we used a biased RW with attraction towards the colony. In order to force the return to the colony, we fixed some terms of the transition matrix, thus ensuring that the sequence of modes alternates first with 'searching', 'foraging' and 'resting', and is then forced to stay in mode 'inbound'. Additionally, we model the effect of the time since departure on the transition probability from 'searching' to 'inbound'.

These state-switching HMMs were fitted to real data according to a maximum likelihood criterion. Fitted models were used to simulate trajectories. The number of modes were defined so that the simulated trajectories would minimize the spectral loss $\mathscr{L}_{\text{spectral}}$ (Equation 4). The initial step was sampled from real data, and we iteratively sampled the next steps, until the trajectory went back to

the colony. In practice, we stopped the simulation once a location was simulated within a 1-km radius around the colony.

Implementation details

GANs were implemented and trained using Pytorch. HMMs were fitted using the momentuHMM r package (McClintock & Michelot, 2018). The code of all the reported experiments is available on our GitHub repository: https://github.com/AmedeeRoy/BirdGAN

3 | RESULTS

3.1 | Architecture selection experiment

Among the four GAN architectures, the fully convolutional GAN led to the best results with better convergence and lowest computation time (Figure 3; Table 2). GANs with LSTM-based discriminators seemed particularly unstable, with highly variable performance through epochs (4). Importantly, only GANs with CNN-based generators managed to simulate looping trajectories. For instance, the 'LSTM-CNN' GAN generated relatively good trajectories with a spectral error $\mathscr{L}_{\text{spectral}}$ lower than 3, yet without being able to loop (Figure 4).

3.2 | GAN versus HMM experiment

On both datasets, GAN and HMM schemes managed to simulate relatively realistic CPFT (see Figure 5). However, the spectral distribution of GAN-derived synthetic trajectories matched the spectral distribution of real trajectories better (Figure 6). In particular, the mean spectral error $\mathscr{L}_{\text{spectral}}$ was about four times smaller, using GANs than using HMMs (Table 3). This was particularly highlighted for the medium frequencies (Figure 6). On the Peruvian dataset, the HMM failed to reproduce spectral features both at lower and higher frequencies (Figure 6a), and on the Brazilian dataset, it failed in the higher frequency range only (Figure 6b). By contrast, HMMs outperformed GANs to sample relevant step distributions (Figure 7).

GAN models capture the real data distribution better, as they can simulate a set of trajectories that share global statistics with the reference dataset. For instance, our synthetic trajectories have consistent trip distance, trip duration and the straightness index distributions (see Figure 7). The straightness index of a trajectory is defined as two times the quotient between the max range to the colony and the trip total distance. The trained GANs also capture spatial information as they reproduce position distributions of observed trajectories (Figure 8; Table 3). GAN-derived synthetic trajectories were indeed mainly heading towards some area of interest (i.e. westward of the colony on the Peruvian dataset, and to the north-east and south-east of the colony on the Brazilian dataset), while HMM-derived trajectories are uniformly spread in all directions around the colony.

4 | DISCUSSION

Deep learning has become the state-of-the-art framework for dealing with a wide range of problems in ecology, such as classification and segmentation tasks, mainly for image analysis (Christin et al., 2019). Despite recent advances in deep learning for the simulation of complex systems, few studies have explored generative models, and particularly GANs to simulate ecological data. To our knowledge, deep convolutional GANs have only been used for data augmentation

TABLE 2 Comparison of GAN architectures. The model with the best performance is shown in bold. Computations have been run using Google Colaboratory resources and relying on Intel(R) Xeon(R) CPU 2.20 GHz

Model	Computation time (min)	$\mathscr{L}_{\text{spectral}}$
CNN-CNN	**1.95**	**0.47**
LSTM-CNN	2.69	1.93
CNN-LSTM	3.03	3.06
LSTM-LSTM	3.59	4.0

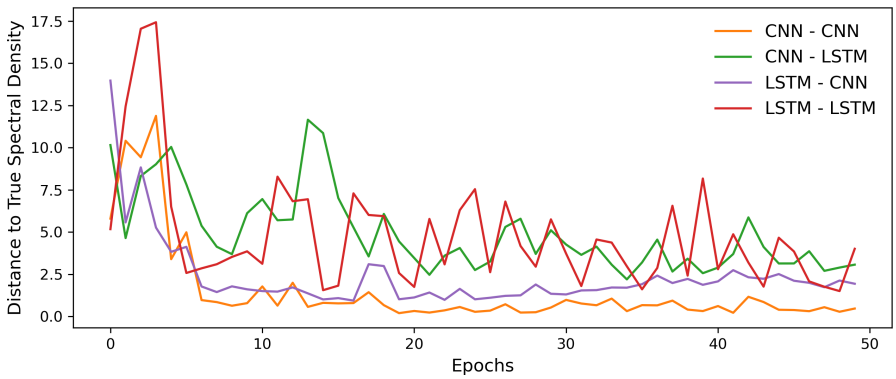

FIGURE 3 Convergence of GAN architecture over 5,000 epochs: The four different GANs correspond to every generator-discriminator pairs. Distance to true spectral density is computed with Equation 4

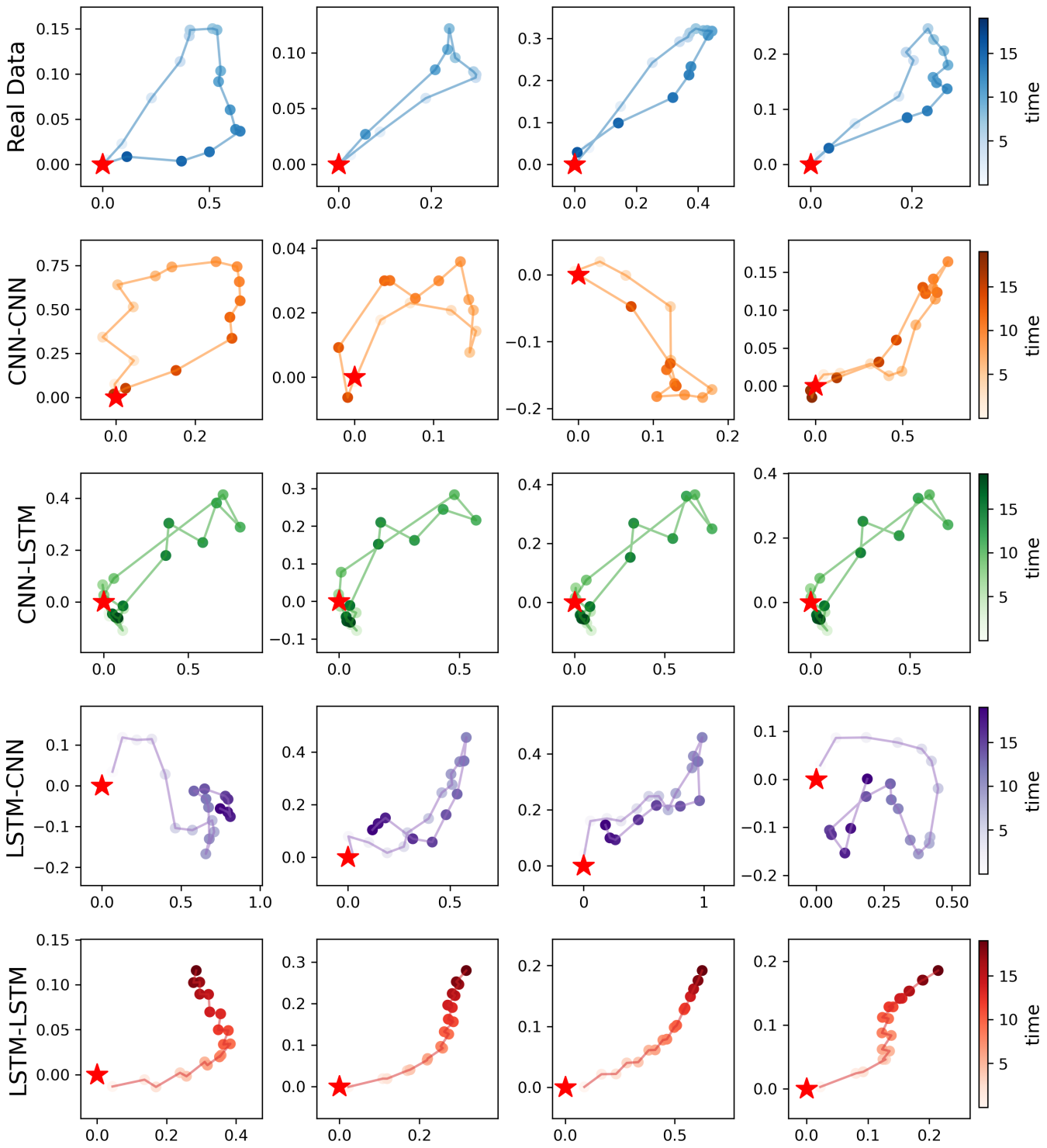

FIGURE 4 Comparison of GAN architectures: Examples of trajectories generated by the architectures tested on the 20-step dataset (see Table 1). The four different GANs correspond to every generator-discriminator pairs

in simulating plant or insect images so far (Lu et al., 2019; Madsen et al., 2019). This study demonstrates that GANs are also promising tools to generate other ecological data, such as animal trajectories.

CPFTs provide an interesting case study in animal movement ecology. Animals performing CPFTs are often supposed to maximize their energy intake rate while travelling away from and back to their central location. Numerous studies have thus investigated how central-place foragers balance their time and energy while foraging (Barraquand et al., 2009; Humphries & Sims, 2014). Capturing the variability of foraging strategies with respect to species, sex or breeding stage is a key element in understanding what drives the decisions of the animals (Phillips et al., 2021). Peruvian boobies *Sula variegata* tracked in this study breed in a highly productive upwelling system, the Humboldt Current System, and feed on relatively

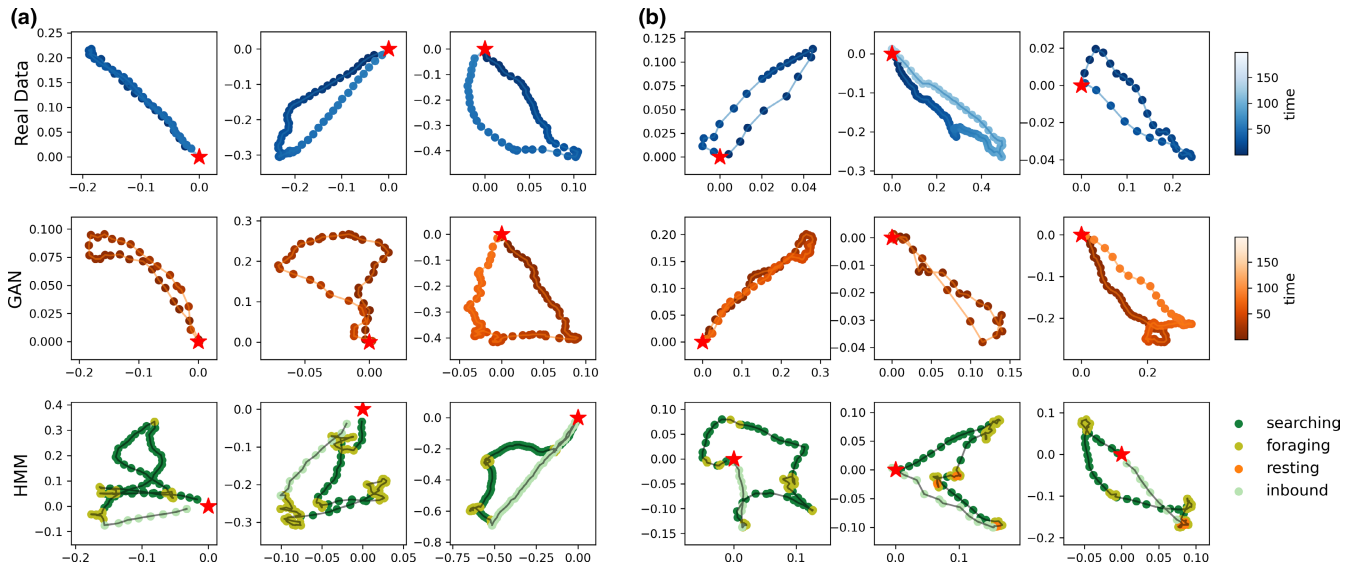

FIGURE 5 GAN versus HMM. Real trajectories used for training are in blue, synthetic trajectories generated by a 'CNN-CNN' GAN are in orange and trajectories generated by HMM are in green. (a) Stands for the 200-step Peruvian dataset and (b) stands for the 200-step Brazilian dataset (see Table 1). All positions at less than 1 km from the colony were removed

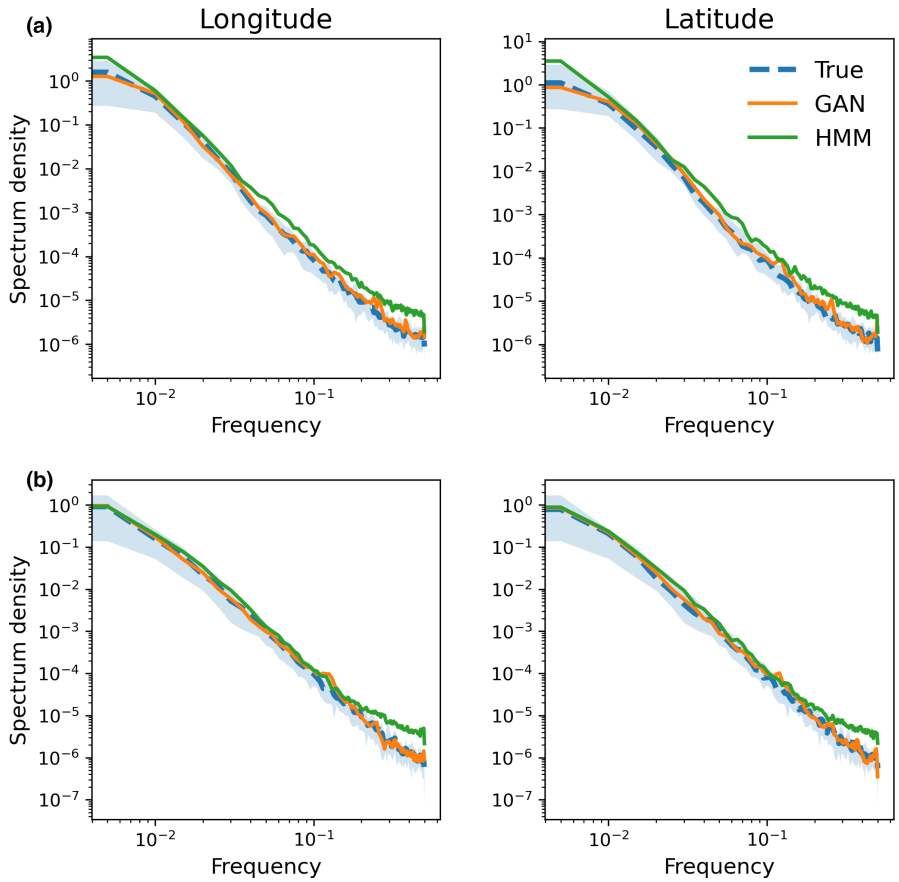

FIGURE 6 GAN versus HMM. Mean Fourier spectrum of real trajectories used for training (blue), and 100 synthetic trajectories generated by a 'CNN-CNN' GAN (orange) and by HMM (green). (a) Stands for the 200-step Peruvian dataset and (b) stands for the 200-step Brazilian dataset (see Table 1)

abundant Peruvian anchovies (Jahncke & Goya, 1998). For these reasons, they performed mainly short foraging trips of about 25 km, eventually travelling up to 75 km at a mean speed of 11 m/s (Figure 7). By contrast, masked boobies breeding at Fernando de Noronha forage mainly in oligotrophic waters (de Santana Campelo et al., 2019). They have to travel way further from their colony during trips of 6–7 hr in average. They also spend substantial time sitting on water in the vicinity of foraging areas.

We demonstrated the great ability of GANs to capture the global statistical properties of these distinct trajectory datasets

derived from seabird species with distinct foraging strategies. By contrast, the current state-of-the-art approaches, such as multistate HMMs, are calibrated at a local scale and are unable to bring out global patterns from these local features. In particular, the use of the behavioural mode 'inbound' relies on the assumption that there is a given time when animals decide to return directly to the colony, which is not always the case. Our numerical experiments pointed out that the relationship between local and global features may be complex for real trajectory data. GANs are explicitly trained so that they best reproduce the characteristic multiscale features of real trajectories. Through strided convolutions, it appears that the considered CNN discriminator overlooks the highest frequencies to focus on large-scale information. Besides, the CNN generator does not explicitly represent a trajectory as a sequential process, which may also impede its ability to reproduce step distribution adequately. This may be a general property of convolution GAN architectures, as they are known not to simulate realistically fine-scale textures in computer vision (Cao et al., 2019).

The simulation of realistic global trajectory patterns can however be of interest for clarifying numerous ecological challenges, and may benefit from GANs through both generator and discriminator networks. Similar to usual RW mixture models, the generator network is a sampler of trajectory data. It could be used to provide null distributions within hypothesis testing frameworks, or within a bootstrap procedure to estimate the uncertainties of features of interest (Michelot et al., 2017). The ability of GANs to reproduce large scale also makes it particularly relevant when estimating the distributions of usual global statistical estimators, such as home range distribution (e.g. Hazen et al., 2021), prey encounter probabilities (e.g. Sims et al., 2006) or foraging area distribution (e.g. Ito et al., 2021). For this reason, it could also provide new means to test energy-related hypotheses of foraging trips and foraging optimality (e.g. Humphries & Sims, 2014). In addition, through the computation of a probability of being a 'realistic' trajectory, the discriminator network provides a metric of data similarity and could be used within comparative study of foraging strategies to assess sex-specific (Lewis et al., 2005) or breeding stage differences (Lerma et al., 2020).

Besides, RWs capture step speed and turning angle distributions and seem more relevant to understand what drives animal decisions at the step level. They have indeed proven useful to evaluate the effect of a heterogeneous landscape, and various external features on animal movement, notably through step-selection function (Signer et al., 2019), mixed effect models (Jonsen et al., 2019) or HMMs whose transition states depend on external covariates (van Beest et al., 2019). Yet, these approaches often struggle when accounting for processes that impact movement patterns at larger spatio-temporal scales. Various extensions of basic state-space models have been proposed to take these into account, for example using hidden semi-Markov models (Langrock et al., 2012) and hierarchical HMMs (Adam et al., 2019; Leos-Barajas et al., 2017). In practice, due to their relative complexity to be implemented and to parametrized, they are rarely used.

Future work should investigate how to combine and take the benefits of both GAN and HMM approaches in order to simulate 'realistic' multiscale animal movement processes. Two research directions naturally come up: modifications to the architectures of generator and discriminator networks, and the exploration of different training frameworks. Regarding the first direction, we may consider the combination of CNN architectures and of HMM-driven or HMM-inspired neural architectures (Lei et al., 2016).

TABLE 3 Properties of GAN and HMM simulations. $\mathscr{L}_{\text{spectral}}$ stands for the mean squared error of the logarithmic Fourier decomposition spectrum presented in Figure 6 and Σ stands for the mean squared error of the position distributions presented in Figure 8. The models with the best performance are shown in bold

Dataset	Model	$\mathscr{L}_{\text{spectral}}$	Σ
(A) Peru	**CNN-CNN**	**0.08**	**1.09**
	HMM	0.91	2.63
(A) Brazil	**CNN-CNN**	**0.07**	**0.03**
	HMM	0.88	0.32

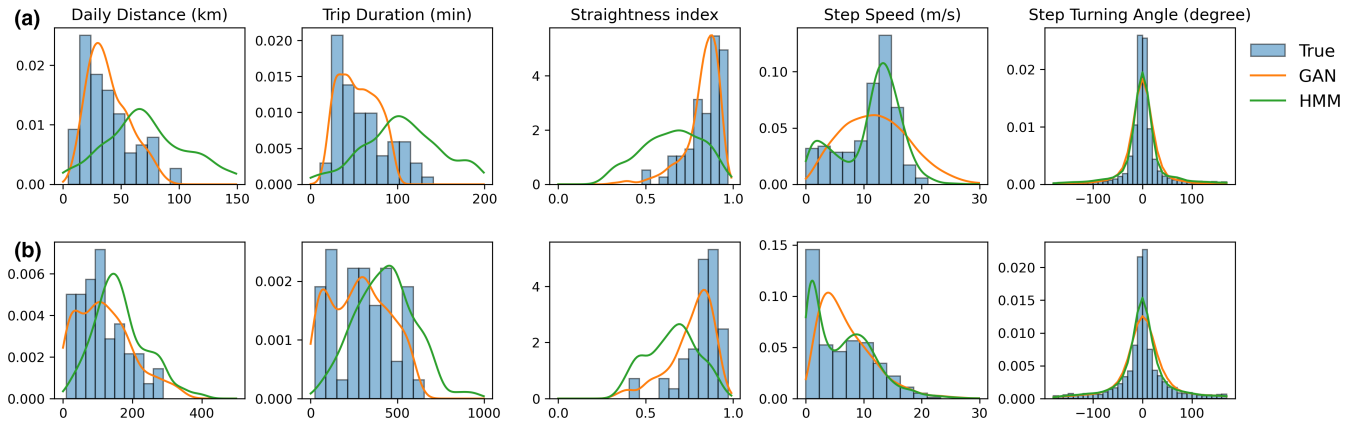

FIGURE 7 GAN versus HMM. Histogram of descriptive statistics derived from real trajectories used for training (blue), 100 synthetic trajectories generated by a 'CNN-CNN' GAN (orange) and by HMM (green). (a) Stands for the 200-step Peruvian dataset and (b) stands for the 200-step Brazilian dataset (see Table 1). The mean squared error of these position distribution estimations are presented in Table 3

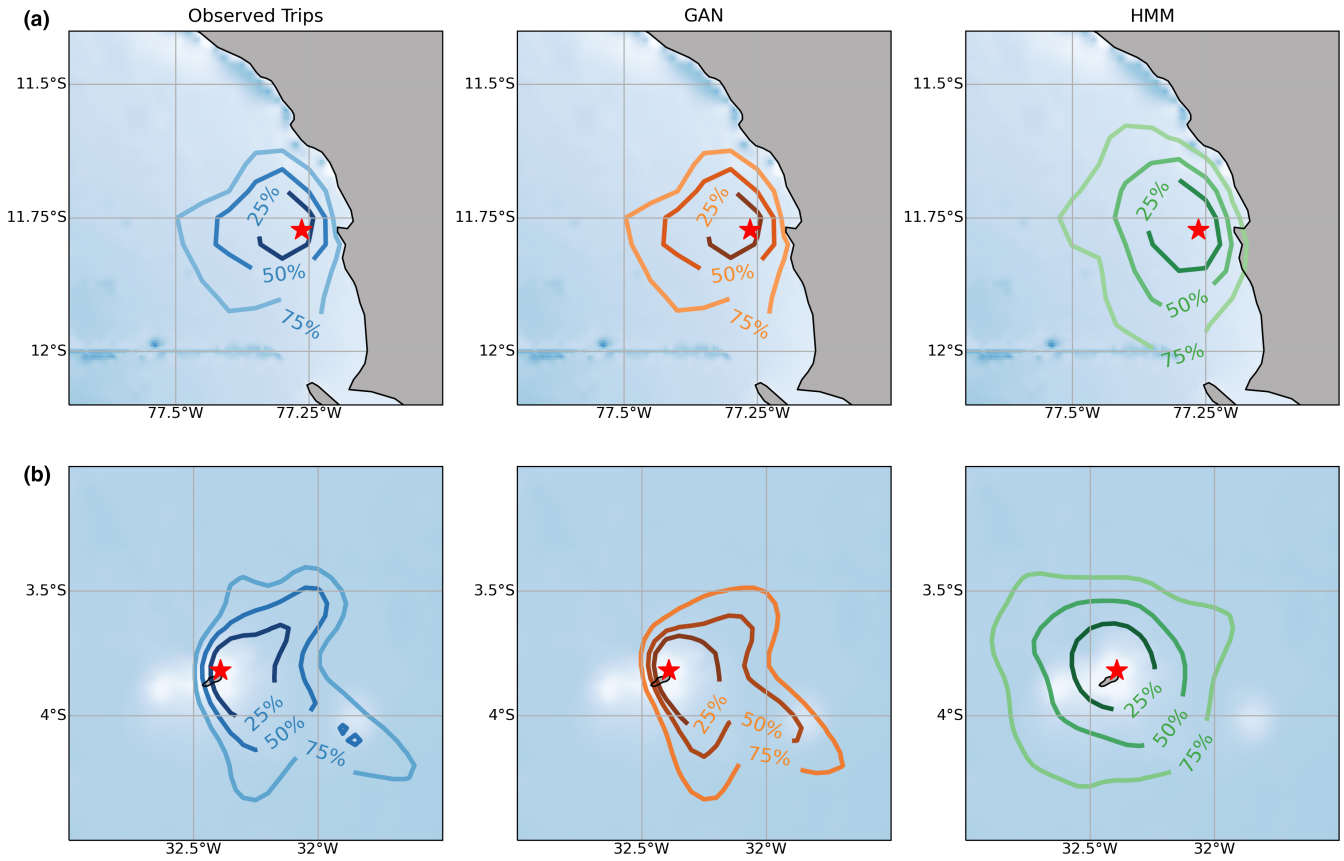

FIGURE 8 GAN versus HMM. Kernel density estimation of position distributions on real trajectories used for training (blue), 100 synthetic trajectories generated by a 'CNN-CNN' GAN (orange) and by HMM (green). (a) Stands for the 200-step Peruvian dataset and (b) stands for the 200-step Brazilian dataset (see Table 1)

Beyond the explicit parameterization of Markovian processes, recurrent architectures such as LSTM seem appealing to embed some latent representation of a behavioural mode sequence, from which one could, for instance, expect to sample the multimodal feature of speed distribution more satisfactorily (Figure 7). Inspired from hierarchical HMM schemes, hierarchical GANs with scale-specific network modules also arise as a relevant direction (Huang et al., 2019). Regarding the training framework, one may first explore different adversarial losses such as the popular Wasserstein GAN (Arjovsky et al., 2017). Though this loss would not lead alone to improvements regarding the simulation of local-scale features, they typically lead to more stable training frameworks, which may be helpful when considering more complex architectures. One could also complement the adversarial loss by a likelihood-based loss derived from a multimodal RW model to explicitly constrain the fine-scale features.

Numerous existing varieties of GANs could also provide great support for movement ecology, especially conditional GAN (Isola et al., 2018). A conditional GAN consists of a GAN with some external variable that conditions its output. One could therefore test for conditions that would explain behavioural variabilities at large scale such as individual characteristics (e.g. sex, mass, breeding stage) or environmental characteristics (e.g. prey distributions, oceanographic features). This typically applies to the assessment of different environmental scenarios and associated animal trajectories, a broad scientific challenge that includes the prediction of the potential impact of climate change on animal behaviour (Hückstädt et al., 2020). Conditional GANs would also provide new means for the interpolation and super-resolution of trajectory data, as performed in computer vision (Ledig et al., 2017).

GANs provide a powerful framework to simulate complex stochastic processes without requiring any specification of a likelihood function; it also frees ecologists from the assumption of first-order Markovianity. This study notably illustrates their ability to reproduce large- to medium-scale property statistics of seabird trajectories when used in their most classical form. It is also an ultra-flexible tool that could further benefit from existing tools, such as HMMs that are calibrated on step distributions, but that usually fail to reproduce large-scale properties. We believe GANs to be a truly promising tool for movement ecology, opening thus new research avenues to simulate and further our understanding of animal trajectories.

ACKNOWLEDGEMENTS

This work is a contribution to the TRIATLAS project (European Union's Horizon 2020 research and innovation program—grant

agreement No. 817578), to the Mixed International Laboratory TAPIOCA Program and to the Young Team IRD Program (JEAI) TABASCO. RF was supported by LEFE program (LEFE MANU project IA-OAC), CNES (grant SWOT-DIEGO) and the ANR Projects Melody and OceaniX. Fieldworks have been conducted thanks to the cooperative agreement between IRD, the Agence Nationale de la Recherche (ANR) project TOPINEME and of the International Joint Laboratory DISCOH. The authors thank all people who conducted fieldwork: H. Weimerskirch, K. Delord, C. Barbraud, Y. Tremblay, J. Silva, G. Passuni, C. Boyd, C. Saraux, A. Brunel, J. Jacoby, L. Figuereido and G. T. Nunes. They thank the Brazilian Ministry of Environment and Fernando de Noronha's firemen for their authorization and technical support to capture seabirds in Brazil. They thank the Ministry of Agriculture of Peru and island guards for their authorization and technical support to capture seabirds in Peru.

CONFLICT OF INTEREST

The authors declare no conflict of interest.

AUTHORS' CONTRIBUTIONS

All authors conceived the ideas. A.R. performed the analysis. All authors contributed to the writing of the article.

PEER REVIEW

The peer review history for this article is available at https://publons.com/publon/10.1111/2041-210X.13853.

DATA AVAILABILITY STATEMENT

All data and codes are available on the GitHub repository accompanying this paper (Roy et al., 2022), and referenced under DOI https://doi.org/10.5281/zenodo.6373812.

ORCID

Amédée Roy https://orcid.org/0000-0003-3047-1463
Ronan Fablet https://orcid.org/0000-0002-6462-423X
Sophie Lanco Bertrand https://orcid.org/0000-0003-1976-3799

ENDNOTE

[1] This subset is referred to as a batch in the deep learning literature.

REFERENCES

Adam, T., Griffiths, C. A., Leos-Barajas, V., Meese, E. N., Lowe, C. G., Blackwell, P. G., Righton, D., & Langrock, R. (2019). Joint modelling of multi-scale animal movement data using hierarchical hidden Markov models. *Methods in Ecology and Evolution*, *10*, 1536–1550.

Alom, M. Z., Taha, T. M., Yakopcic, C., Westberg, S., Sidike, P., Nasrin, M. S., Hasan, M., Van Essen, B. C., Awwal, A. A. S., & Asari, V. K. (2019). A state-of-the-art survey on deep learning theory and architectures. *Electronics*, *8*, 292.

Arjovsky, M., Chintala, S., & Bottou, L. (2017). Wasserstein generative adversarial networks. Proceedings of the 34th International Conference on Machine Learning, PMLR 70:214-223.

Barraquand, F., Inchausti, P., & Bretagnolle, V. (2009). Cognitive abilities of a central place forager interact with prey spatial aggregation in their effect on intake rate. *Animal Behaviour*, *78*, 505–514.

Bastos, R., Martins, B., Cabral, J. A., Ceia, F. R., Ramos, J. A., Paiva, V. H., Luís, A., & Santos, M. (2020). Oceans of stimuli: An individual-based model to assess the role of olfactory cues and local enhancement in seabirds' foraging behaviour. *Animal Cognition*, *23*, 629–642.

Bergman, C. M., Schaefer, J. A., & Luttich, S. N. (2000). Caribou movement as a correlated random walk. *Oecologia*, *123*, 364–374.

Boyd, C., Grünbaum, D., Hunt, G. L., Punt, A. E., Weimerskirch, H., & Bertrand, S. (2017). Effects of variation in the abundance and distribution of prey on the foraging success of central place foragers. *Journal of Applied Ecology*, *54*(5), 1362–1372. https://doi.org/10.1111/1365-2664.12832

Cao, Y. J., Jia, L. L., Chen, Y. X., Lin, N., Yang, C., Zhang, B., Liu, Z., Li, X. X., & Dai, H. H. (2019). Recent advances of generative adversarial networks in computer vision. *IEEE Access*, *7*, 14985–15006.

Christin, S., Hervet, É., & Lecomte, N. (2019). Applications for deep learning in ecology. *Methods in Ecology and Evolution*, *10*, 1632–1644.

Chung, H., Lee, J., & Lee, W. Y. (2021). A review: Marine bio-logging of animal behaviour and ocean environments. *Ocean Science Journal*, *56*(2), 117–131. https://doi.org/10.1007/s12601-021-00015-1

Codling, E. A., Plank, M. J., & Benhamou, S. (2008). Random walk models in biology. *Journal of the Royal Society Interface*, *5*, 813–834.

de Santana Campelo, R. P., Bonou, F. K., de Melo Júnior, M., Diaz, X. F. G., Bezerra, L. E. A., & Neumann-Leitão, S. (2019). Zooplankton biomass around marine protected islands in the tropical Atlantic Ocean. *Journal of Sea Research*, *154*, 101810. https://doi.org/10.1016/j.seares.2019.101810

DeAngelis, D. L., & Grimm, V. (2014). Individual-based models in ecology after four decades. *F1000Prime Reports*, *6*, 39.

Durall, R., Keuper, M., & Keuper, J. (2020). Watch your up-convolution: CNN based generative deep neural networks are failing to reproduce spectral distributions. Proceedings of the IEEE/CVF Conference on Computer Vision and Pattern Recognition (CVPR), 7890–7899.

Esteban, C., Hyland, S. L., & Rätsch, G. (2017). Real-valued (medical) time series generation with recurrent conditional GANs. arXiv preprint arXiv:170602633.

Gao, N., Xue, H., Shao, W., Zhao, S., Qin, K. K., Prabowo, A., Rahaman, M. S., & Salim, F. D. (2020). Generative adversarial networks for Spatio-temporal data: A survey. arXiv preprint arXiv:200808903.

Goodfellow, I. J., Pouget-Abadie, J., Mirza, M., Xu, B., Warde-Farley, D., Ozair, S., Courville, A., & Bengio, Y. (2014). Generative adversarial networks. Advances in neural information processing systems, 27.

Grimm, V., Revilla, E., Berger, U., Jeltsch, F., Mooij, W. M., Railsback, S. F., Thulke, H. H., Weiner, J., Wiegand, T., & DeAngelis, D. L. (2005). Pattern-oriented modeling of agent-based complex systems: Lessons from ecology. *Science*, *310*, 987–991.

Hartig, F., Calabrese, J. M., Reineking, B., Wiegand, T., & Huth, A. (2011). Statistical inference for stochastic simulation models - theory and application. *Ecology Letters*, *14*(8), 816–827. https://doi.org/10.1111/j.1461-0248.2011.01640.x

Hazen, E. L., Abrahms, B., Brodie, S., Carroll, G., Welch, H., & Bograd, S. J. (2021). Where did they not go? Considerations for generating pseudo-absences for telemetry-based habitat models. *Movement Ecology*, *9*, 5.

Huang, H., Zhang, F., Zhou, Y., Yin, Q., & Hu, W. (2019). High resolution SAR image synthesis with hierarchical generative adversarial networks. IGARSS 2019 - IEEE International Geoscience and Remote Sensing Symposium, 2782–2785.

Hückstädt, L. A., Piñones, A., Palacios, D. M., McDonald, B. I., Dinniman, M. S., Hofmann, E. E., Burns, J. M., Crocker, D. E., & Costa, D. P. (2020). Projected shifts in the foraging habitat of crabeater seals along the Antarctic Peninsula. *Nature Climate Change*, *10*, 472–477.

Humphries, N. E., & Sims, D. W. (2014). Optimal foraging strategies: Lévy walks balance searching and patch exploitation under a very broad range of conditions. *Journal of Theoretical Biology*, *358*, 179–193.

Isola, P., Zhu, J. Y., Zhou, T., & Efros, A. A. (2017). Image-to-image translation with conditional adversarial networks. Proceedings of the IEEE Conference on Computer Vision and Pattern Recognition (CVPR), 1125–1134.

Ito, K., Watanabe, Y. Y., Kokubun, N., & Takahashi, A. (2021). Inter-colony foraging area segregation quantified in small colonies of Adélie Penguins. *Ibis*, *163*(1), 90–98. https://doi.org/10.1111/ibi.12837

Jahncke, J., & Goya, E. (1998). Diets of the Guanay cormorant and Peruvian booby as indicators of the abundance and distribution of anchovy. *Boletin Instituto del Mar del Peru*, *17*, 15–33.

Johnson, D. S., London, J. M., Lea, M. A., & Durban, J. W. (2008). Continuous-time correlated random walk model for animal telemetry data. *Ecology*, *89*, 1208–1215.

Jonsen, I. D., McMahon, C. R., Patterson, T. A., Auger-Méthé, M., Harcourt, R., Hindell, M. A., & Bestley, S. (2019). Movement responses to environment: Fast inference of variation among southern elephant seals with a mixed effects model. *Ecology*, *100*, e02566.

Kays, R., Crofoot, M. C., Jetz, W., & Wikelski, M. (2015). Terrestrial animal tracking as an eye on life and planet. *Science*, *348*, aaa2478.

Langrock, R., King, R., Matthiopoulos, J., Thomas, L., Fortin, D., & Morales, J. M. (2012). Flexible and practical modeling of animal telemetry data: Hidden Markov models and extensions. *Ecology*, *93*, 2336–2342.

LeCun, Y., Bengio, Y., & Hinton, G. (2015). Deep learning. *Nature*, *521*, 436–444.

Ledig, C., Theis, L., Huszar, F., Caballero, J., Cunningham, A., Acosta, A., Aitken, A., Tejani, A., Totz, J., Wang, Z.. & Shi, W. (2017). Photo-realistic single image super-resolution using a generative adversarial network. Proceedings of the IEEE Conference on Computer Vision and Pattern Recognition (CVPR), 4681–4690.

Lei, J., Li, G., Zhang, J., Guo, Q., & Tu, D. (2016). Continuous action segmentation and recognition using hybrid convolutional neural network-hidden Markov model model. *IET Computer Vision*, *10*, 537–544.

Leos-Barajas, V., Photopoulou, T., Langrock, R., Patterson, T. A., Watanabe, Y. Y., Murgatroyd, M., & Papastamatiou, Y. P. (2017). Analysis of animal accelerometer data using hidden Markov models. *Methods in Ecology and Evolution*, *8*, 161–173.

Lerma, M., Dehnhard, N., Luna-Jorquera, G., Voigt, C. C., & Garthe, S. (2020). Breeding stage, not sex, affects foraging characteristics in masked boobies at Rapa Nui. *Behavioral Ecology and Sociobiology*, *74*(12). https://doi.org/10.1007/s00265-020-02921-1

Lewis, S., Schreiber, E. A., Daunt, F., Schenk, G. A., Orr, K., Adams, A., Wanless, S., & Hamer, K. C. (2005). Sex-specific foraging behaviour in tropical boobies: Does size matter?. *Ibis*, *147*(2), 408–414. https://doi.org/10.1111/j.1474-919x.2005.00428.x

Lu, C. Y., Arcega Rustia, D. J., & Lin, T. T. (2019). Generative adversarial network based image augmentation for insect Pest classification enhancement. *IFAC-PapersOnLine*, *52*, 1–5.

Madsen, S. L., Dyrmann, M., Jørgensen, R. N., & Karstoft, H. (2019). Generating artificial images of plant seedlings using generative adversarial networks. *Biosystems Engineering*, *187*, 147–159.

Malde, K., Handegard, N. O., Eikvil, L., & Salberg, A. B. (2020). Machine intelligence and the data-driven future of marine science. *ICES Journal of Marine Science*, *77*, 1274–1285.

Massardier-Galatà, L., Morinay, J., Bailleul, F., Wajnberg, E., Guinet, C., & Coquillard, P. (2017). Breeding success of a marine central place forager in the context of climate change: A modeling approach. *PLoS ONE*, *12*, e0173797.

McClintock, B. T., Johnson, D. S., Hooten, M. B., Hoef, J. M. V., & Morales, J. M. (2014). When to be discrete: The importance of time formulation in understanding animal movement. *Movement Ecology*, *2*, 21.

McClintock, B. T., King, R., Thomas, L., Matthiopoulos, J., McConnell, B. J., & Morales, J. M. (2012). A general discrete-time modeling framework for animal movement using multistate random walks. *Ecological Monographs*, *82*, 335–349.

McClintock, B. T., & Michelot, T. (2018). momentuHMM: R package for generalized hidden Markov models of animal movement. *Methods in Ecology and Evolution*, *9*(6), 1518–1530. https://doi.org/10.1111/2041-210x.12995

McMahon, L. A., Rachlow, J. L., Shipley, L. A., Forbey, J. S., Johnson, T. R., & Olsoy, P. J. (2017). Evaluation of micro-GPS receivers for tracking small-bodied mammals. *PLoS ONE*, *12*, e0173185.

Michelot, T., & Blackwell, P. G. (2019). State-switching continuous-time correlated random walks. *Methods in Ecology and Evolution*, *10*(5), 637–649. https://doi.org/10.1111/2041-210x.13154

Michelot, T., Langrock, R., Bestley, S., Jonsen, I. D., Photopoulou, T., & Patterson, T. A. (2017). Estimation and simulation of foraging trips in land-based marine predators. *Ecology*, *98*, 1932–1944.

Morales, J. M., Haydon, D. T., Frair, J., Holsinger, K. E., & Fryxell, J. M. (2004). Extracting more out of relocation data: Building movement models as mixtures of random walks. *Ecology*, *85*, 2436–2445.

Nathan, R., Getz, W. M., Revilla, E., Holyoak, M., Kadmon, R., Saltz, D., & Smouse, P. E. (2008). A movement ecology paradigm for unifying organismal movement research. *Proceedings of the National Academy of Sciences of the United States of America*, *105*, 19052–19059.

Patterson, T., Thomas, L., Wilcox, C., Ovaskainen, O., & Matthiopoulos, J. (2008). State-space models of individual animal movement. *Trends in Ecology & Evolution*, *23*, 87–94.

Phillips, J. A., Fayet, A. L., Guilford, T., Manco, F., Warwick-Evans, V., & Trathan, P. (2021). Foraging conditions for breeding penguins improve with distance from colony and progression of the breeding season at the South Orkney Islands. *Movement Ecology*, *9*, 22.

Pirotta, E., Edwards, E. W. J., New, L., & Thompson, P. M. (2018). Central place foragers and moving stimuli: A hidden-state model to discriminate the processes affecting movement. *Journal of Animal Ecology*, *87*, 1116–1125.

Radford, A., Metz, L., & Chintala, S. (2015). Unsupervised representation learning with deep convolutional generative adversarial networks. arXiv preprint. arXiv.1511.06434.

Ropert-Coudert, Y., Beaulieu, M., Hanuise, N., & Kato, A. (2009). Diving into the world of biologging. *Endangered Species Research*, *10*, 21–27.

Roy, A., Fablet, R., & Lanco Bertrand, S. (2022). AmedeeRoy/BirdGAN: BirdGAN (v1.0). *Zenodo*, https://doi.org/10.5281/zenodo.6373812

Sequeira, A. M. M., Heupel, M. R., Lea, M. A., Eguíluz, V. M., Duarte, C. M., Meekan, M. G., Thums, M., Calich, H. J., Carmichael, R. H., Costa, D. P., Ferreira, L. C., Fernandéz-Gracia, J., Harcourt, R., Harrison, A. L., Jonsen, I., McMahon, C. R., Sims, D. W., Wilson, R. P., & Hays, G. C. (2019). The importance of sample size in marine megafauna tagging studies. *Ecological Applications*, *29*, e01947.

Signer, J., Fieberg, J., & Avgar, T. (2019). Animal movement tools (amt): R package for managing tracking data and conducting habitat selection analyses. *Ecology and Evolution*, *9*, 880–890.

Sims, D. W., Witt, M. J., Richardson, A. J., Southall, E. J., & Metcalfe, J. D. (2006). Encounter success of free-ranging marine predator movements across a dynamic prey landscape. *Proceedings of the Royal Society B: Biological Sciences*, *273*, 1195–1201.

van Beest, F. M., Mews, S., Elkenkamp, S., Schuhmann, P., Tsolak, D., Wobbe, T., Bartolino, V., Bastardie, F., Dietz, R., von Dorrien, C., Galatius, A., Karlsson, O., McConnell, B., Nabe-Nielsen, J., Olsen, M. T., Teilmann, J., & Langrock, R. (2019). Classifying grey seal behaviour in relation to environmental variability and commercial fishing activity—A multivariate hidden Markov model. *Scientific Reports*, *9*, 5642.

Viswanathan, G. M., Raposo, E. P., & da Luz M. G. E. (2008). Lévy flights and superdiffusion in the context of biological encounters and random searches. *Physics of Life Reviews*, *5*(3), 133–150. https://doi.org/10.1016/j.plrev.2008.03.002

Winner, K., Noonan, M. J., Fleming, C. H., Olson, K. A., Mueller, T., Sheldon, D., & Calabrese, J. M. (2018). Statistical inference for home range overlap. *Methods in Ecology and Evolution*, *9*, 1679–1691.

Ylitalo, A. -K., Heikkinen, J., & Kojola, I. (2021). Analysis of central place foraging behaviour of wolves using hidden Markov models. *Ethology*, *127*(2), 145–157. https://doi.org/10.1111/eth.13106

Yoda, K. (2019). Advances in bio-logging techniques and their application to study navigation in wild seabirds. *Advanced Robotics*, *33*, 108–117.

Zurell, D., Berger, U., Cabral, J. S., Jeltsch, F., Meynard, C. N., Münkemüller, T., Nehrbass, N., Pagel, J., Reineking, B., Schröder, B., & Grimm, V. (2010). The virtual ecologist approach: Simulating data and observers. *Oikos*, *119*, 622–635.

How to cite this article: Roy, A., Fablet, R. & Bertrand, S. L. (2022). Using generative adversarial networks (GAN) to simulate central-place foraging trajectories. *Methods in Ecology and Evolution*, *13*, 1275–1287. https://doi.org/10.1111/2041-210X.13853